Journal of Applied Biological Sciences
E-ISSN: 2146-0108 15(3): 294-309, 2021
Research Article

EFFECT OF *IN-VITRO* AND *IN-VIVO* MODELS OF DIABETES ON AKT PATHWAY IN PERIPHERAL BLOOD LYMPHOCYTES

Melinda Nongbet Sohlang*, Suktilang Majaw

Department of Biotechnology and Bioinformatics, North-Eastern Hill University, Shillong, 793022, Meghalaya, India

**Corresponding Author:*
E-mail: smajaw2021@gmail.com

(Received 20th October 2020; accepted 07th March 2021)

ABSTRACT. In this study, we investigated the effect of *in-vitro* and *in-vivo* models of diabetes on AKT phosphorylation and its downstream targets. For the *in-vitro* model, peripheral blood lymphocytes (PBL) were incubated with high glucose (Glc) or palmitic acid (PA) concentrations while for the *in-vivo* model, PBL was isolated from alloxan-induced diabetic mice. PBL was then examined for triglyceride content, lipid accumulation, enzyme activities, and phosphorylation state of AKT, glycogen synthase kinase-3β (GSK3β) and voltage-gated anion channel (VDAC). CD4/CD8 ratio and pro-inflammatory profile were monitored as indicators of lymphocyte function. Glc-/PA-exposed PBL demonstrated increased triglyceride content and lipid droplets. This was accompanied by increased acetyl CoA carboxylase and decreased carnitine palmitoyltransferase activity while glycogen synthase activity was unchanged. Glc- and PA-exposed PBL showed decreased pAKT-, pGSK3β-protein expression. Interestingly, relative to pVDAC expression, Glc- and PA-exposed PBL showed contrasting results. An altered CD4/CD8 ratio with elevated pro-inflammatory profile was noted indicating impaired lymphocyte function. Results of the *in-vivo* model were consistent with those of cultured PBL except the data of pVDAC expression showed resemblance to those of Glc-incubated PBL. These results demonstrate that diabetic conditions can reduce the expression of AKT and its downstream targets, GSK3β which might contribute to impaired lymphocyte function. Contrasting results on pVDAC expression under high Glc and PA suggests the possible involvement of other candidate substrates downstream to GSK3β.

Keywords: *Diabetes, glucose, palmitic acid, GSK3β, VDAC*

INTRODUCTION

Nutrients such as glucose and fatty acid play crucial roles in immune signaling and immune cell functions [1]. Imbalance in these nutrients can disrupt the fate of immune cells as noticed in a range of diseases. Diabetes is a disease with elevated circulating glucose and free fatty acids known to harm immune cells [2, 3] including lymphocytes [4, 5]. Impaired lymphocyte function has been linked to changes in lymphocyte metabolism in a study on alloxan-induced diabetes [4].

Lymphocytes homeostasis requires the coordination of various signaling pathways involved in metabolic processes. AKT signaling pathway is fundamentally important as it controls nutrient uptake and cellular metabolism. AKT is a serine/threonine kinase that functions mostly by phosphorylating downstream targets such as other protein kinases, apoptotic proteins, and transcription factors [6, 7]. Additionally, it regulates glycogen synthase kinase3β (GSK3β) protein which in turn phosphorylate other proteins such as voltage-dependent anion channel (VDAC). VDAC is present at the outer mitochondrial

membrane and has a task of transporting metabolites to enable the mitochondria to maintain membrane potential. Adverse changes in mitochondrial membrane potential are disadvantageous to cell metabolism and can even lead to death [8]. Besides, GSK3β has been identified as a key mediator of pro-inflammatory cytokine production [9, 10].

Disruption of AKT pathways has been linked to cellular dysfunction and numerous diabetic complications [11, 12, 13]. Although in diabetes, glucose and palmitic acid levels are high, their levels might be variable due to various physiological and endocrine factors. Therefore, we designed *in-vitro* experiments to determine lymphocyte dysfunction induced by glucose (Glc) or palmitic acid (PA) overload in peripheral blood lymphocytes (PBL) isolated from mice. In the present study, we investigated the effect of *in-vitro* and *in-vivo* diabetes on AKT phosphorylation and its downstream targets in peripheral blood lymphocytes isolated from mice.

MATERIALS AND METHODS

Reagents

Alloxan monohydrate, histopaque-1077, palmitic acid, bovine serum albumin, and protease inhibitor cocktail were purchased from Sigma, USA. RPMI-1640, fetal bovine serum, phytohemagglutinin were purchased from Gibco, USA. Protein A/G-Sepharose was from Abcam, USA, nitrocellulose membrane (0.2 um), chemiluminescence substrate was from Bio-Rad, USA. Glucose was from Himedia, India while other chemicals and reagents of analytical grade were from Himedia, India, and Sisco Research Laboratories, India.

Animal

Male Swiss albino mice (25-30 g) were procured from Pasteur Institute, Shillong, and acclimatized for 7 days before experimentation. The mice were housed under standard conditions of 22°C, 12:12 h dark and light cycle, fed water, and standard pelleted diet *ad libitum*. Institutional Ethical Clearance (dated 15th December, 2015) was obtained for conducting the experiments on the mice model.

Peripheral blood lymphocytes isolation

Mice blood was collected retro-orbitally into heparin tubes, diluted with phosphate buffer saline (PBS, pH 7.2), and then loaded to histopaque-1077 following which the tubes were centrifuged at 800rpm for 15min. The peripheral blood lymphocytes (PBL) cell layer was then collected and washed twice in PBS [14].

In-vitro experimental design

Isolated PBL (1 x 10^6 cells) are cultured in RPMI-1640 medium containing glucose (Gibco, cat no. 11875093) at 37°C in a 5% CO_2 incubator. The medium was supplemented with 10% fetal bovine serum, 100 U/ml streptomycin, 200 U/ml penicillin, phytohemagglutinin, and either with 40 mM (Glc) [15] or 150 μM (PA) [16] for 72 h to mimic conditions of hyperglycemia/ hyperlipidemia respectively.

Preparation of palmitic acid

Palmitic acid was prepared as a stock solution of 100 mM dissolved in 100 % ethanol at 70°C. This solution was complexed with Bovine serum albumin (BSA) by shaking for 1 h at 50°C [17]. The fatty acid to BSA molar ratio was at 3:1 [18]. To normalize the effect of the solvents used to dissolve PA, control groups received the same volume of ethanol-BSA in the absence of PA.

Media D-glucose concentration for in-vitro model

The medium glucose concentration for the *in-vitro* model was determined by the coupled enzyme activities of horseradish peroxidase and glucose oxidase [19]. 10 µl of the medium was analyzed in a 1ml total reaction volume containing 1.75 mM each of 4-aminoantipyrine and N-ethyl-N-sulfopropyl-m-toluidine as the chromophore solution, 120 mM sodium phosphate, pH 6.0, 2.7 U/ml HRP. The reaction was started by the addition of 1.6 U/ml glucose oxidase. The solution was left to stand for 45-60 min at 25 °C before taking the absorbance reading at λ550 nm. The concentration was calculated from the standard curve made using D-glucose at varying concentrations.

In-vivo experimental design

Peripheral blood lymphocytes isolated from alloxan-induced diabetic mice was used as the *in-vivo* model. Diabetes (blood glucose level <200 mg/dl) was induced by injecting alloxan monohydrate (Sigma, USA, cat no. A7413-25G) intravenously at a dose of 60 mg/kg b.w. [20] dissolved in sodium acetate buffer (0.15 M, pH 4.5) [21]. An equal volume of the buffer was injected into normal control mice. On the 7^{th} day, blood was collected for isolation of PBL [4].

Intraperitoneal Glucose tolerance test (IPGTT), intraperitoneal insulin tolerance test (IPITT), and measurement of insulin level for diabetic mice

Mice were fasted for 16 h before conducting these two experiments. To conduct IPGTT, mice were administered with glucose (2 mg/kg b.w.) intraperitoneally (i.p.). Following injection, blood glucose level was estimated at 0, 30, 60, and 120 min by using a standard glucometer. For IPITT, insulin (0.75 U/kg b.w) was administered *via* the i.p. route followed by blood glucose level measurement at 0, 30, 60, 120 min. The total area under the curve (AUC) which is the average of the total of blood glucose in two different time intervals was calculated for blood glucose level representation [22]. Insulin was quantified in mU/L using experimental kits according to the manufacturer's instructions (Fine Test, China, cat no. EM0260).

Lipid accumulation determined using Oil red O stain and by measuring intracellular triglyceride (TG) level for in-vitro and in-vivo models

Lipid accumulation

Isolated PBL were washed in PBS, fixed in 4% paraformaldehyde for 10 min at room temperature. The formaldehyde was discarded, cells washed, and incubated for another 1 h. The fixative was then washed with distilled water followed by a 60 % isopropanol wash for 5 min at room temperature. The PBL was then smeared onto slides and air-dried at room temperature. Slides were then stained with Oil red O (0.5% w/v stock solution prepared in 95% isopropyl alcohol) for 15 min and counterstained with hematoxylin. The

excess stain from slides was removed using distilled water, then mounted on an aqueous mounting medium, and PBL with red positively stained lipid droplets (in %) are counted immediately [23].

Intracellular triglyceride

Intracellular triglyceride (TG) level (in mmol/L) was quantified according to the manufacturer's instruction using a triglyceride kit (Abcam, cat no. ab65336). Briefly, isolated PBL from *in vitro* and *in vivo* models were washed with PBS and homogenized in 1 ml of NP40. The samples were then heated to 80°C in a water bath until the NP40 becomes cloudy. This was then cooled down to room temperature and centrifuged for 2 min. 50 µL of sample and standard was then added to sample and standard wells respectively. 2 µL of lipase and assay buffer each was added to all the wells and incubated for 20 min at room temperature. Next 50 µL of TG mix (containing assay buffer, TG probe, and TG enzyme mix) was added to all the wells and mixed properly. After a 60 min incubation in the dark, the output was measured in a microplate reader (Bio-Rad 680 Plate reader) at λ570 nm.

Enzymes activities determination for in-vitro and in-vivo models

Mitochondrial fraction preparation for Carnitine palmitoyltransferase (CPT) assay

Peripheral blood lymphocytes was incubated for 10 min in RSB-hypo buffer containing a 1% protease inhibitor cocktail and swollen cells disrupted using Dounce homogenizer [24]. 1.5 mL of the homogenized mixture was immediately mixed with 2.5X mitochondrial isolation buffer (525 mM mannitol, 175 mM sucrose, 12.5 mM tris, 2.5 mM EDTA, pH 7.5) followed by centrifugation at 1300 g for 10 min at 4°C. The supernatant was then centrifuged at 17000 g for 15 min. The resulting mitochondrial pellet was resuspended in buffer (70 mM sucrose, 220 mM mannitol, 2 mM HEPES, 1 mM EDTA, pH7.4).

CPT assay

Assay (A) contains 116 mM Tris, pH 8, 1.1 mM EDTA, 0.035 mM palmitoyl CoA, 0.12 mM DTNB, 0.1% TritonX-100, 1.1 mM l(-)-carnitine and 100 µl of the sample. Assay (B) contains the reaction mix without l(-)-carnitine. The assay which started with the addition of the sample follows the release of free CoA from palmitoyl CoA using the reagent 5, 5'-dithiobis(2-nitobenzoate) (DTNB) at λ412 nm. The difference in reaction rates for assay A and B equates to CPT activity [25, 26].

Preparation of homogenized sample for acetyl coenzyme A carboxylase (ACC) and glycogen synthase (GS) assay

Peripheral blood lymphocytes was homogenized in ice-cold buffer (20 mM Tris, 150 mM KH_2PO_4, 5 mM EDTA, 10 mM monothioglycerol, pH 7.8) and centrifuged at 12,000 g for 10 min at 4 °C. The supernatant was used for assaying ACC and GS activity at λ340 nm in a spectrophotometer (Hitachi U2910, Japan).

ACC and GS assay

Assay mixture for ACC contained 50 mM Tris, 10 mM potassium citrate, 10 mM $MgCl_2$,1mg/ml BSA, 3.75 mM ATP, 0.125 mM acetyl CoA, 25 mM $KHCO_3$, 0.5 mM PEP, 0.125 mM NADH, 5.6 U pyruvate kinase, 5.6 U lactate dehydrogenase and 10 µL homogenate [27]. GS reaction mixture consisted of 50 mM Tris, 12.5 mM $MgCl_2$, 1 mM

EDTA, 0.75 mM UDP-glucose, 1 % glycogen, 0.7 mM PEP, 7.5 U pyruvate kinase, 15 U lactate dehydrogenase, 7.1 mM NADH and 10 µl sample [28].

All enzyme activities are represented as U/mg protein where 1 catalyzes the conversion of 1 µmol substrate into the product at a given assay condition. Protein concentration was estimated using Bradford's method [29].

$CD4^+/CD8^+$ measurement for in-vitro and in-vivo models

Flow cytometry for phenotype analysis was done in FACS Calibur (BD Bioscience, USA) where $1x10^6$ PBL was counted using trypan blue in a hemocytometer and were stained with fluorescent-conjugated antibodies (CD4-FITC and CD8-PE). Ten thousand events were collected in a forward/side scatter and the result was analyzed using CellQuest Pro (BD Bioscience). The lymphocyte subsets data are presented as a ratio of $CD4^+/CD8^+$ cell percentages.

Cytokine profile for in-vitro and in-vivo models

The cytokine profile for the *in-vivo* model was carried out using mouse serum. For the *in vitro* model, released cytokines were measured by taking 100 µl of culture media at the end of the 72h culture period. Tumor necrosis factor-α (TNF-α) and interleukin-6 (IL-6) levels were estimated using the TNF-α mouse ELISA kit (Invitrogen, cat no. KMC3011) and the IL-6 mouse ELISA kit (Cayman Chemical, cat no. 583371) respectively according to the manufacturer's instruction at λ450nm. The result was expressed as pg/ml.

Western blot for in-vitro and in-vivo models

Cells were lysed with buffer containing 10mM HEPES, 5 mM NaCl, 1mM dithiothreitol, protease inhibitor, pH 7.5, and centrifuged at 12000 g for 5 min at 4°C. Protein content was determined using Bradford's method. Western blotting was performed using a primary antibody against pAKT (S473) (1:1000, CST, USA) and p-GSK3β (S21/9) (1:1000, CST) followed by incubation with secondary antibody conjugated to HRP (1:40000, CST). Target proteins were quantified relative to β-actin (1:1000, Abcam) as the internal control protein. Protein bands were visualized by enhanced chemiluminescence (BioRad, USA) and band intensity was calculated using the BioRad Image Lab 5.0 software.

For studying pVDAC expression level, the mitochondrial fraction was immunoprecipitated with VDAC (1:1000, Abcam, cat no. ab14734) antibody and protein A/G agarose beads overnight at 4ºC which was later probed with p-(S/T) Phe antibody (1:1000, CST, cat no. 9631S) in a western blot experiment. The p-(S/T) Phe antibody detects the phosphorylated serine or threonine on the immunoprecipitated protein while remaining non-reactive with the non-phosphorylated form.

Statistical analysis

Results were expressed as mean±SEM analyzed using Student t-test on GraphPad Prism 7 with *$p<0.05$, **$p<0.01$, and ***$p<0.001$ values considered as statistically significant concerning their respective controls.

RESULTS AND DISCUSSION

IPGTT, IPITT, and measurement of insulin level for diabetic mice

Area under the curve values serve as a good indicator of the host tolerance to glucose and sensitivity towards insulin performed as IPGTT and IPITT respectively [21]. The total AUC taken from 0 to 120 min for both IPGTT (Fig.1A**)** and IPITT (Fig. 1B) showed higher blood glucose for diabetic mice when compared to the control. Further, diabetic mice also showed decreased serum insulin levels ($p<0.01$) (Fig. 2C). These results are characteristics associated with diabetes as observed in other studies [30, 31].

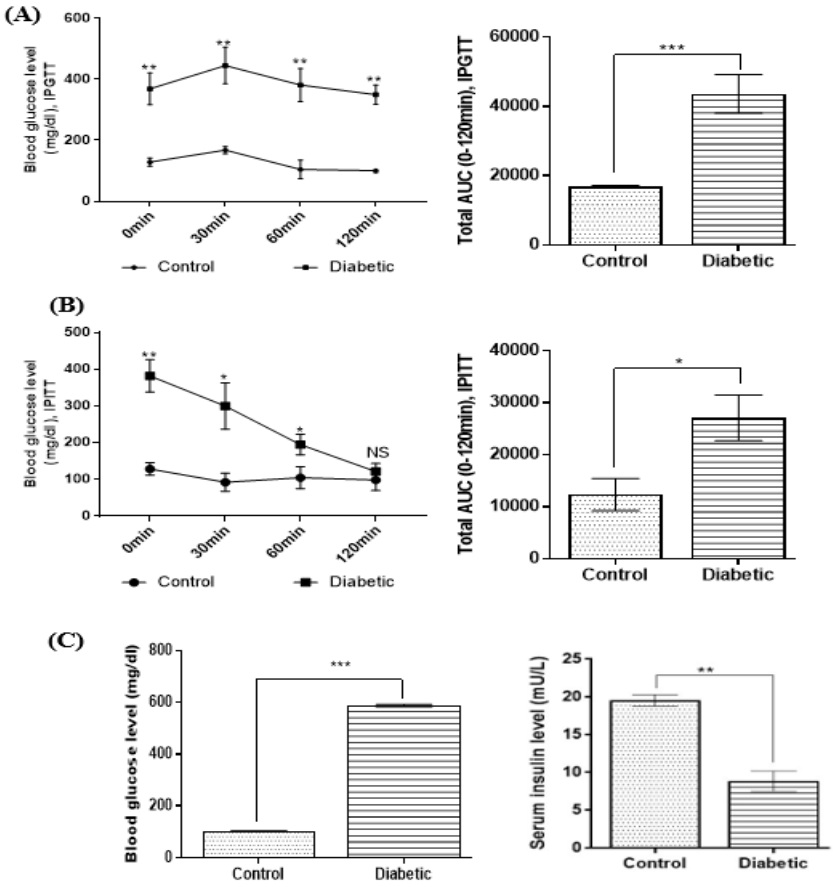

Fig 1*. Effect of alloxan-diabetes on (A) intraperitoneal glucose tolerance test (IPGTT); (B) intraperitoneal insulin tolerance test (IPITT); (C) blood glucose level (n=6) and (D) serum insulin of mice (n=3). Data presented as mean ± SEM, p<*0.05, **<0.01, ***<0.001 versus respective control.*

Lipid accumulation, intracellular triglycerides in PBL of in-vitro and in-vivo models

Peripheral blood lymphocytes contained lipid droplets that are positive for Oil Red O, an oil-soluble colorant as opposed to control cells that instead take up the hematoxylin, a basic dye causing the PBL to stain blue. These lipid droplets are cytoplasmic and membrane-associated in location [23] as represented by a black arrow in Fig. 2A. Out of 100 cells that were counted, the number of positively stained cells was more ($p<0.001$) in Glc/PA treated cells than in control (Fig. 2B). The isolated diabetic PBL also showed

accumulated lipid droplets when stained with Oil Red O ($p<0.001$) (Fig. 2B). Lipid deposition was further quantified by measuring the intracellular triglyceride (TG) level. As observed in Fig. 2C**,** TG levels increased significantly ($p<0.01$) when compared to the respective control.

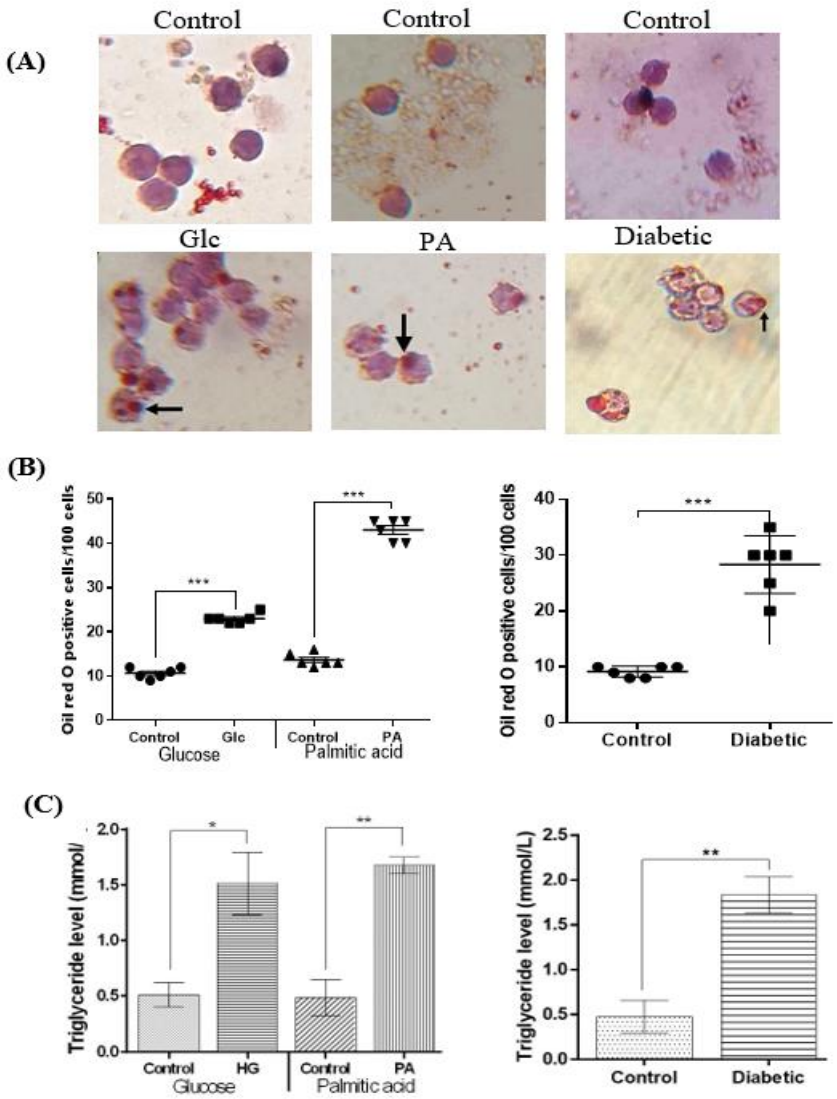

Fig 2. *Lipid accumulation in PBL from in-vitro and in-vivo groups: (A) Oil Red O dye accumulation in PBL observed morphologically under the microscope (100X). The black arrow indicates lipid droplets. (B) Oil Red O positive cells (n=6). (C) Intracellular triglyceride content (n=3). Data presented as mean ± SEM, p<*0.05, **<0.01, ***<0.001 versus respective controls.*

Enzymes activities in PBL of in-vitro and in-vivo models

Fig. 3A showed an increased ACC enzyme activity ($p<0.001$) for Glc/PA-exposed PBL and PBL of diabetic mice as compared to control. CPT activity was found to decrease in Glc-/PA-treated PBL ($p<0.01$; $p<0.001$) and in PBL isolated from diabetic mice ($p<0.001$) as compared to their respective control (Fig. 3B). The changes in these

enzyme activities suggest that high Glc/PA can inhibit fatty acid oxidation while promoting *de novo* synthesis [32]. No significant difference in GS activity was observed in the cultured and diabetic PBL when compared with their respective controls (Fig. 3C).

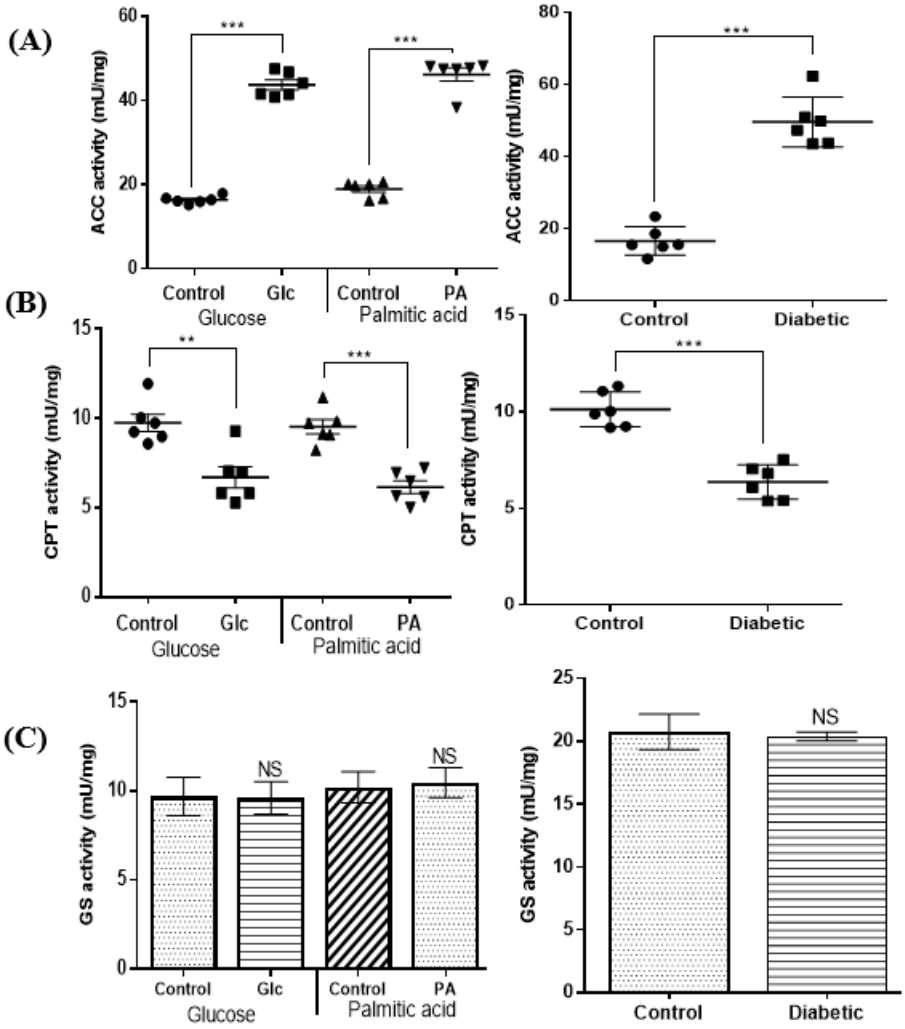

***Fig 3**. Enzyme activities of PBL from in-vitro and in-vivo groups: (A) Acetyl coenzyme A carboxylase (ACC); (B) Carnitine palmitoyltransferase (CPT); (C) Glycogen synthase (GS). Data presented as mean ± SEM (n=6), NS, not significant versus respective controls.*

Lymphocyte subsets and cytokine production for in-vitro and in-vivo models

A fluctuation in FFA or glucose levels has been reported to affect lymphocyte proliferation and balance [33]. Lipid abnormalities and hyperglycemia are associated with elevated pro-inflammatory cytokines viz., IL-6, and TNF-α concentration [34, 35]. In our study, $CD4^+/CD8^+$ ratio decreases under high Glc ($p<0.05$), high PA (0.001) and in diabetic ($p<0.01$) groups respective to the controls (Fig. 4A). Furthermore, all the treatment conditions elevated the TNF-α ($p<0.05$) (Fig. 4B) and IL-6 levels for Glc/PA ($p<0.05$) including the diabetic group ($p<0.01$) compared to their respective controls (Fig. 4C).

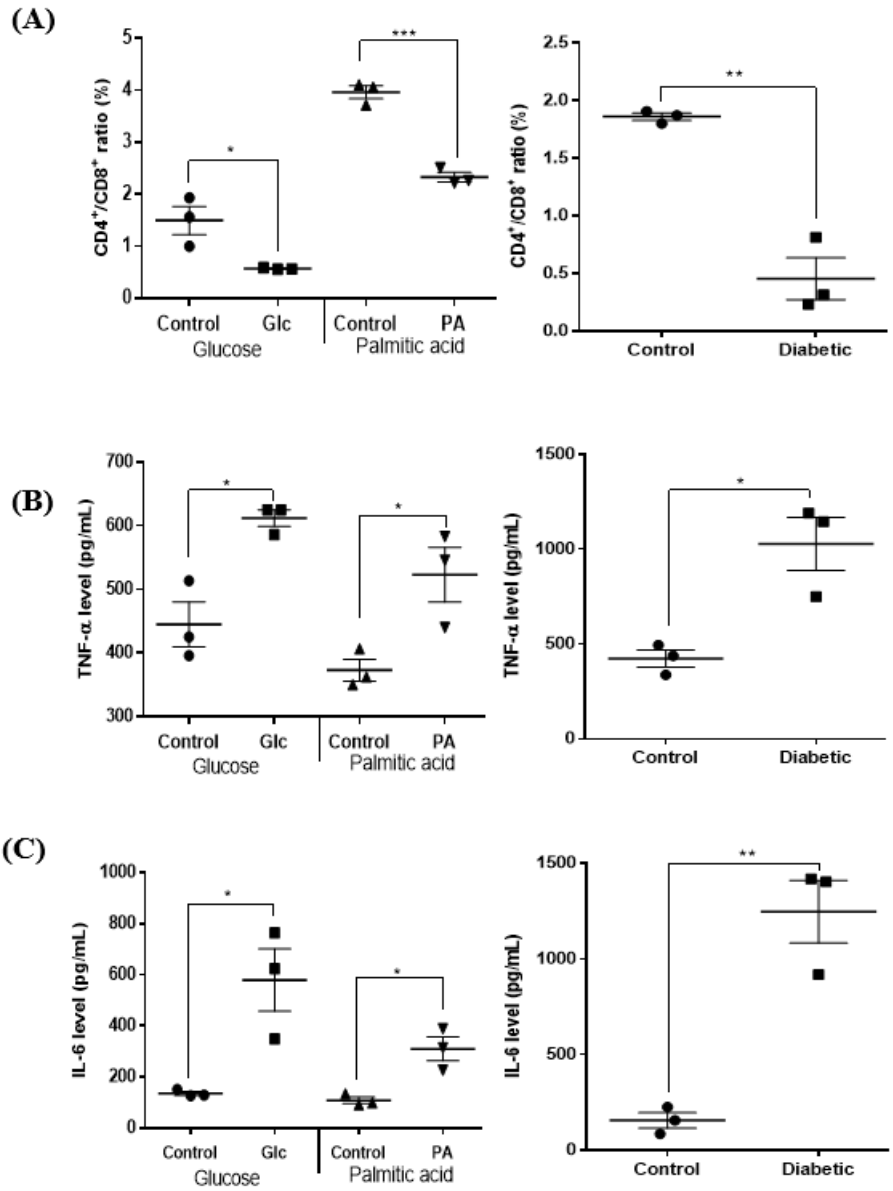

Fig 4. *Effect of in-vitro/ in-vivo diabetic condition on lymphocyte subset and cytokines production: (A) CD4⁺/CD8⁺cell ratio; (B) Tumor necrosis factor-α (TNF-α); (C) Interleukin-6 (IL-6). Data presented as mean ± SEM (n=3), p<*0.05, **<0.01, ***<0.001 versus respective controls.*

Protein expression in PBL of in-vitro and in-vivo models

To understand the mechanism behind the effect of high Glc/PA on PBL function, expression of AKT, and its downstream effectors, GSK3β was investigated. In the current study, PBL of in-vitro and in-vivo models showed decreased pAKT ($p<0.05$) and decreased phosphorylated GSK3β protein expression when compared to their respective control (Fig.5A-B). GSK3β is known to be responsible for phosphorylation of VDAC, an outer mitochondrial protein involved in metabolites flux and apoptosis [36]. Our result showed an increase in phosphorylated VDAC protein expression ($p<0.01$) in PBL treated

with Glc and from diabetic mice while no change was observed under the PA treated group (Fig.5C).

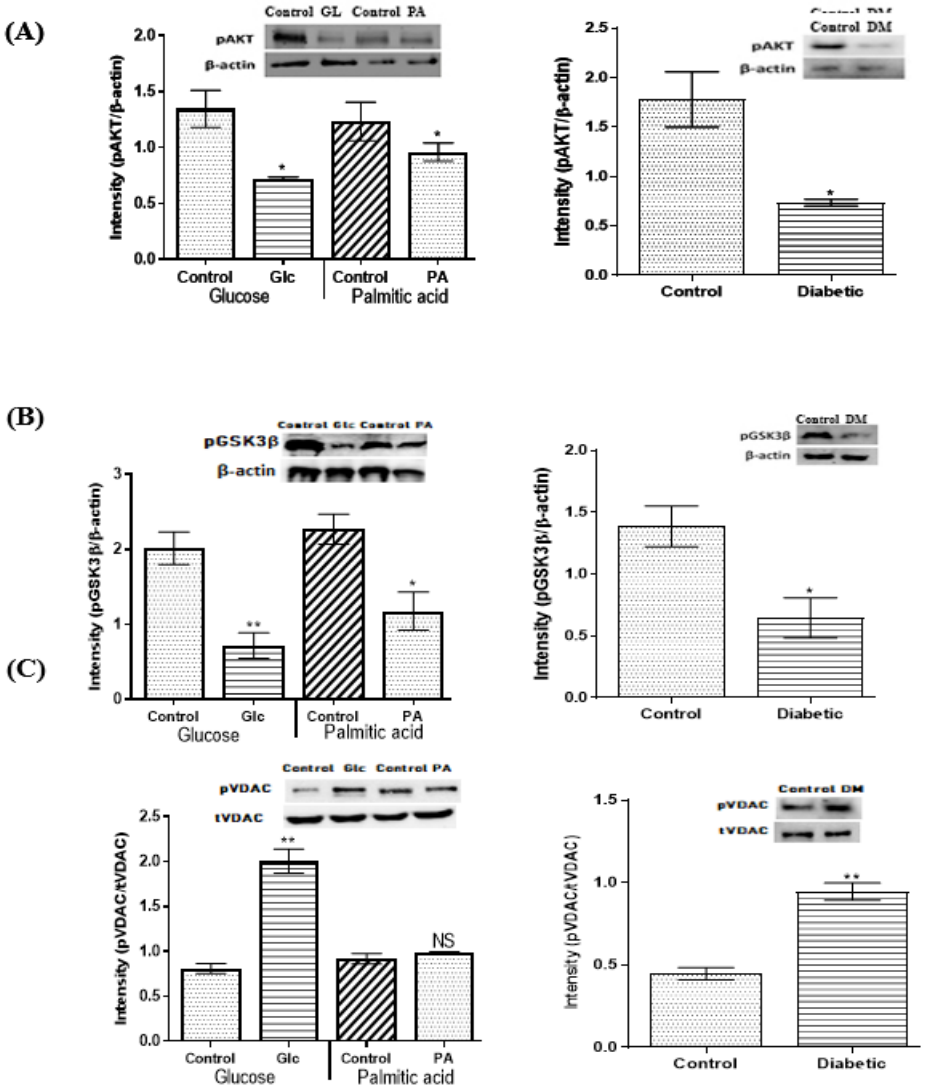

Fig 5. *Effect of in-vitro/ in-vivo diabetic condition on phosphorylated protein expression: (A) AKT; (B) Glycogen synthase kinase-3β (GSK-3β); (C) Voltage-dependent anion channel (VDAC). Data presented as mean ± SEM (n=3), p<*0.05, **<0.01, ***<0.001, NS, not significant versus respective controls where, Glc: 40 mM Glucose/ PA: 150 µM palmitic acid; DM: diabetic.*

This study demonstrates the effect of *in-vitro* and *in-vivo* diabetes on the function of PBL mediated *via* AKT and its downstream targets. PBL of the *in-vitro* model was incubated in culture media with high Glc/ PA which represents conditions of hyperglycemia and hyperlipidemia observed in diabetes. Recreation of diabetes environment *in-vitro* is crucial for studying the effect of diabetes as these models are governed not only by the cells themselves but also by the conditions they are exposed to [37]. As seen in other studies, incubation of PBL under high glucose/ palmitic acid concentration mimics the *in-vitro* milieu of diabetes [5, 16, 38]. For the *in-vivo* model,

PBL were isolated from a diabetic group which showed characteristically high blood glucose level, glucose intolerance, and insulin insensitivity.

Peripheral blood lymphocytes from both the *in-vitro* and *in-vivo* groups showed increased lipid deposition and intracellular TG levels. ACC, a lipogenic enzyme was higher in PBL of both the studied models as supported by other studies under high glucose [39], high PA [40] and diabetes [41]. Further, this increased in ACC activity may have acted as an inhibitor of CPT thereby decreasing its activity in PBL as reported elsewhere [42, 43]. Therefore, impaired metabolism indicated by reduced CPT enzyme associated with β-oxidation and lipogenic ACC upregulation may have contributed to the increased lipid deposition [44, 40, 45]. ACC and CPT play key roles in fatty acid metabolism and as previously reported evidence indicate that changes in basic cellular lipid metabolism have critical effects on T cell proliferation and cell fate decisions [46]. In the study performed by Bhutada et al. [47], glycogen synthesis has been shown to compete with triglyceride synthesis despite that these pathways are distant in the cellular metabolic network. Therefore, we investigated the effect of the treatment conditions on the GS activity of PBL. The low or no glycogen store in lymphocytes [48, 49] might have contributed to GS activity remaining unchanged in all the treatment groups as compared to their respective control observed in our study.

AKT activation through its phosphorylation enables it to mediate downstream responses by further phosphorylating a range of intracellular proteins [50]. The protein expression level of phosphorylated AKT was markedly reduced in PBL under Glc/ PA and isolated from diabetic mice. Studies such as in high glucose-induced endothelial cells [51], PA-induced C2C12 myotubes [52], and in diabetes [12, 13] have demonstrated reduced pAKT expression. Consequently, GSK3β phosphorylation would be expected to decrease. GSK3β phosphorylation at Ser9 or Ser389 leads to its inactivation. pGSK3β may have contributed to TG and lipid accumulation by regulating ACC and other lipogenic enzyme gene expression as seen in the muscle cells [53] and the diabetic cardiac tissue [54].

AKT/ GSK3β closely relates to the abnormal activation and proliferation of lymphocytes in other disease conditions including diabetes [55]. In our study, the helper/ cytotoxic lymphocyte ratio [56] and inflammatory profile [57] parameters for assessing immune function were monitored. The phosphorylated state of AKT/ GSK3β in our study may have contributed to the changes in the lymphocyte function. Our data revealed a decreased $CD4^+$/ $CD8^+$ ratio as suggested in previous studies [57, 58, 59]. This may be due to the reduction of lymphocyte migration/ maturation at the secondary lymphoid organs or a failed T cell growth accompanied by decreased pAKT and pGSK3β [7, 60]. Our study also reported a shift towards a pro-inflammatory profile indicated by an increase in TNF-α and IL-6 levels in all treatment conditions. Elevated TNF-α and IL-6 levels have been reported in alloxan-induced diabetes [57] including in other cells lines exposed to palmitic acid [61, 62] and high glucose [63, 64]. Reduced pAKT and pGSK3β accompanied these changes in the inflammatory profile [65, 66]. AKT/ GSK3β phosphorylation state may therefore, influence lymphocyte function.

GSK3β has been reported to phosphorylate many proteins including VDAC, an outer mitochondrial protein. VDAC regulates cell metabolism by mediating the cytosol-mitochondria metabolite flux and by interacting with other proteins at the mitochondrial membrane [36]. One of them is the CPT protein responsible for uptake and oxidation of chain fatty acid through the ACSL1-CPT1a-VDAC complex [67, 68]. However, the impact of VDAC phosphorylation or dephosphorylation on immune function has not

clearly elucidated. In our study, Glc and diabetes increase VDAC phosphorylation while in PA-induced PBL, the VDAC phosphorylation state remains close to normal.

CONCLUSION

In our study *in-vitro* and *in-vivo* diabetes inhibited Akt/GSK3β phosphorylation and caused dysregulation in the PBL function. We found contrasting results for downstream targets of GSK3β in PBL exposed to high Glc and high PA. Further characterization of phosphorylation sites would be needed to connect the downstream targets of GSK3β with immune dysfunction under diabetic condition. In conclusion, our data suggest that aberrant states of AKT phosphorylation may have the potential to alter lymphocyte function in diabetes.

Acknowledgement. We thank the Department of Biotechnology & Bioinformatics, North-Eastern Hill University for providing the research facility and fianacial support through various grants received by the department which includes: Non-plan (FA2/NP/Allocation/2018-19 dated 13.08.2018), UGC-SAP (F4-7/2016/DRS-I (SAP-II) dated 28.04.2016), DBT-M.Sc. Teaching Program (102/IFD/DBT/SAN/2140/2006-07 dated 16.03.2017), DST-FIST (SR/FSI/LSI-666/2016(C) dated 15.12.2017). During this period Melinda N. Sohlang received a DBT-JRF fellowship from the Department of Biotechnology, Government of India, New Delhi. The authors donot have a conflict of interest.

REFERENCES

[1] Walls, J., Sinclair, L., Finlay, D. (2016): Nutrient Sensing, Signal Transduction and Immune Responses. Seminars in Immunology 28: 396-407. doi: 10.1016/J.Smim.2016.09.001.

[2] Grill, V., Bjorklund, A. (2000): Dysfunctional Insulin Secretion in Type 2 Diabetes: Role of Metabolic Abnormalities. Cellular and Molecular Life Sciences 57: 429-440. doi 10.10007/PL00000705.

[3] Unger, R. H. (1995): Lipotoxicity in the Pathogenesis of Obesity-Dependent NIDDM. Genetic and Clinical Implications. Diabetes 44: 863-870. doi: 10.2337/Diab.44.8.863

[4] Otton, R., Mendonça, J. R., Curi, R. (2002): Diabetes Causes Marked Changes in Lymphocyte Metabolism. Journal of Endocrinology 174: 55-61.

[5] Takahashi, H. K, Cambiaghi, T. D., Luchessi, A. D., Hirabara, S. M., Vinolo, M. A., Newholme, P., Curi, R. (2012): Activation of Survival and Apoptotic Signaling Pathways in Lymphocytes Exposed to Palmitic Acid. Journal of Cellular Physiology 227: 339-350.

[6] Franke, T. F., Hornik, C. P., Segev, L., Shostak, G. A., Sugimoto, C. (2003): PI3K/AKT and Apoptosis: Size Matters. Oncogene 22: 8983-8998.

[7] Badr, G., Ramadan, N. K., Abdel-Tawab, H. S., Ahmed, S. F., Mahmoud, M. H. (2018): Camel Whey Protein Protects Lymphocytes from Apoptosis *via* the PI3K-AKT, NF-KB, ATF-3, and Hsp-70 Signalling Pathway in Heat-Stressed Male Mice. Biochemistry and Cell Biology 96: 407-416. doi: 10.1139/bcb-2017-0217.

[8] O'Rourke, B. (2007): Mitochondrial Ion Channels. Annual Review of Physiology 69: 19-49.

[9] Martin, M., Rehani, K., Jope, R. S., Michalek, S. M. (2005): Toll-Like Receptor—Mediated Cytokine Production is Differentially Regulated by Glycogen Synthase Kinase 3. Nature Immunology 6: 777-784.

[10] Hu, X., Paik, P. K., Chen, J., Yarilina, A., Kockeritz, L., Lu, T. T., Woodgett, J. R., Ivashkiv, L. B. (2006): IFN-γ Suppresses IL-10 Production and Synergizes with TLR2 by Regulating GSK3 and CREB/AP-1 Proteins. Immunity 24: 563-574. doi: 10.1016/J.Immuni.2006.02.014

[11] Zdychova, J., Komers, R. (2005): Emerging Role of AKT Kinase/Protein Kinase B Signaling in Pathophysiology of Diabetes and its Complications. Physiological Research 54: 1-16.

[12] Cozzone, D., Frojdo, S., Disse, E., Debard, C., Laville, M., Pirola, L., Vidal, H. (2008): Isoform-Specific Defects of Insulin Stimulation of Akt/Protein Kinase B (PKB) in Skeletal Muscle Cells from Type 2 Diabetic Patients. Diabetologia 51: 512-521. doi: 10.1007/s00125-007-0913-8.

[13] Sun, D., Shen, M., Li, J., Li, W., Zhang, Y., Zhao, L., Zhang, Z., Yuan, Y., Wang, H., Cao, F. (2011): Cardioprotective Effects of Tanshinone IIA Pretreatment *via* Kinin B2 Receptor-Akt-GSK-3β Dependent Pathway in Experimental Diabetic Cardiomyopathy. Cardiovascular Diabetology 10: 4. doi: 10.1186/1475-2840-10-4.

[14] Liu, F. C., Hoyt, D. B., Coimbra, R., Junger, W. G. (1996): Proliferation Assays with Human, Rabbit, Rat, and Mouse Lymphocytes. *In Vitro* Cellular & Developmental Biology- Animal 32: 520-523. doi: 10.1007/BF02722976.

[15] Oleszczak, B., Szablewski, L., Pliszka, M. (2012): The Effect of Hyperglycemia and Hypoglycemia on Glucose Transport and Expression of Glucose Transporters in Human Lymphocytes B and T: An In Vitro Study. Diabetes Research and Clinical Practice 96:170-178. doi: 10.1016/j.diabres.2011.12.012.

[16] Mu, Y. M., Yanase, T., Nishi, Y., Tanaka, A., Saito, M., Jin, C., Mukasa, C., Okabe, T., Nomura, M., Goto, K., Nawata, H. (2001): Saturated FFAs, Palmitic Acid and Stearic Acid, Induce Apoptosis in Human Granuloma Cells. Endocrinology 142: 3590-3597. doi: 10.1210/endo.142.8.8293

[17] Yuan, Z., Cao, A., Liu, H., Guo, H., Zang, Y., Wang, Y., Wang, H., Yin, P., Peng, W. (2017): Calcium Uptake v*ia* Mitochondrial Uniporter Contributes to Palmitic Acid–Induced Apoptosis in Mouse Podocytes. Journal of Cellular Biochemistry 118: 2809-2818. doi: 10.1002/jcb.25930.

[18] Rakatzi, I., Mueller, H., Ritzeler, O., Tennagels, N., Eckel, J. (2004): Adiponectin Counteracts Cytokine– and Fatty Acid–Induced Apoptosis in the Pancreatic Beta–Cell Line Ins–1. Diabetologia 47: 249-258. doi: 10.1007/s00125-003-1293-3.

[19] Blake, D. A., Mclean, N. V. (1989): A Colorimetric Assay for the Measurement of D-Glucose Consumption by Cultured Cells. Analytical Biochemistry 177: 156-160. doi: 10.1016/0003-2697(89)90031-6.

[20] Rabeque, C. S., Padmavathy, S. (2013): Hypoglycaemic Effect of *Syzygium caryophyllatum* (L.) Alston on Alloxan Induced Diabetic Albino Mice. Asian Journal of Pharmaceutical and Clinical Research,6: 203-205.

[21] Syiem, D., Syngai, G., Khup, P. Z., Khongwir, B. S., Kharbuli, B., Kayang, H. (2002): Hypoglycemic Effects of *Potentilla fulgens* L. in Normal and Alloxan-Induced Diabetic Mice. Journal of Ethnopharmacology 83: 55-61. doi: 10.1016/s0378-8741(02)00190-3.

[22] Nath, S., Ghosh, S. K., Choudhury, Y. (2017): A Murine Model of Type 2 Diabetes Mellitus Developed Using a Combination of High Fat Diet and Multiple Low Doses of Streptozotocin Treatment Mimics the Metabolic Characteristics of Type 2 Diabetes Mellitus in Humans. Journal of Pharmacological and Toxicological Methods 84: 20-30. doi: 10.1016/j.vascn.2016.10.007.

[23] Delikatny, E. J, Van Holst Pellekaan, C. J., King, N. J. (2001): Autologous Lymphocyte-Monocyte Co-Culture Increases Nmr-Visible and Cytoplasmic Lipids in the Absence of Increased Markers of Lymphocyte Activation. Biochimica Biophysica Acta 1533: 243-254. doi.org/10.1016/S1388-1981(01)00157-3.

[24] Clayton, D. A., Shadel, G. S. (2014): Isolation of Mitochondria from Tissue Culture Cells. Cold Spring Harbour Protocol 2014: 1109-1111. Doi: 10.1101/pdb.prot080002.

[25] Bieber, L., Abraham, T., Helmrath, T. (1972): A Rapid Spectrophotometric Assay for Carnithine Palmitoyl Transferase. Analytical Biochemistry 50: 509-518. doi: 10.1016/0003-2697(72)90061-9.

[26] Markwell, M. K., Mcgroarty, E. J., Bieber, L., Tolbert, N. E. (1973): The Subcellular Distribution of Carnitine Acyltransferases in Mammalian Liver and Kidney. Journal of Biological Chemistry 248: 3426-3432.

[27] Tanabe, T., Nakanishi, S., Hashimoto, T., Ogiwara, H., Nikawa J., Numa, S. (1981): Acetyl-CoA carboxylase from rat liver. Methods in Enzymology 71 Pt C: 5-16. doi: 10.1016/0076-6879(81)71003-6.

[28] Danforth, W. H. (1965): Glycogen Synthetase Activity in Skeletal Muscle. Interconversion of Two Forms and Control of Glycogen Synthesis. Journal of Biological Chemistry 240: 588-593.

[29] Bradford, M. M. (1976): A Rapid and Sensitive Method for the Quantification of Microgram Quantities of Protein Utilizing the Principle of Protein-Dye Binding. Analytical Biochemistry 72: 248-254. doi: 10.1006/abio.1976.9999.

[30] Syiem, D., Khup, P. Z., Syiem, A. B. (2009): Effects of *Potentilla fulgens* Linn. on Carbohydrate and Lipid Profiles in Diabetic Mice. Pharmacologyonline 2: 787-795.

[31] Rynjah, C. V., Boruah, P., Majaw, S. (2016): Evaluation of Hypoglycemic and Antihyperglycemic Effect of Aqueous-Methanolic Leaves Extract of Two Medicinal Plants of Meghalaya in Mice. International Journal of Pharmcological Research 6: 256-263. doi.org/10.7439/ijpr.v6i7.3329.

[32] Liu, J., Yi- Zhang, C., Song, L., Zhang, L., Yang, F., Zhu, X., Cheng, Z., Cao, X., Yang, J. (2019): Nifuroxazide Ameliorates Lipid and Glucose Metabolism in Palmitate-Induced HepG2 Cells. RSC Advances 9: 39394. doi.org/10.1039/C9RA06527J.

[33] Miya, A., Nakamura, A., Miyoshi, H., Takano, Y., Sunagoya, K., Hayasaka, K., Shimizu, C., Terauchi, Y., Atsumi, T. (2018): Impact of Glucose Loading on Variations in CD4+ and CD8+ T Cells in Japanese Participants with or without Type 2 Diabetes. Frontiers in Endocrinology 9: 81. doi: 10.3389/fendo.2018.00081.

[34] Pickup, J. C., Mattock, M. B., Chusney, G. D., Burt, D. (2007): NIDDM as a Disease of the Innate Immune System: Association of Acute-Phase Reactant and Interleukin-6 with Metabolic Syndrome X. Diabetologia 40: 1286–1292. doi: 10.1007/s001250050822.

[35] Gonzalez, Y., Herrera, M. T., Soldevila, G., Garcia-Garcia, L., Fabian, G., Pereez-Armendariz, E. M., Bobadilla, K., Guzman- Beltran, S., Sada, E., Torres, M. (2012): High Glucose Concentrations Induce TNF-α Production Through the Down-Regulation of CD33 in Primary Human Monocytes. BMC Immunology 13: 19. doi: 10.1186/1471-2172-13-19.

[36] Pastorino, J. G., Hoek, J. B., Shulga, N. (2005): Activation of Glycogen Synthase Kinase 3β Disrupts the Binding of Hexokinase II to Mitochondria by Phosphorylating Voltage Dependent Anion Channel and Potentiates Chemotherapy-Induced Cytotoxicity. Cancer Research 65: 10545–10554. doi: 10.1158/0008-5472.CAN-05-1925.

[37] Lilao-Garzon, J., Valverde-Tercedor, C., Munoz-Descalzo, S., Brito-Casillas, Y., Wagner, A. M. (2020): In Vivo and In Vitro Models of Diabetes: A Focus on Pregnancy. In: Advances in Experimental Medicine and Biology. Springer, New York, NY. doi.org/10.1007/5584_2020_536.

[38] Vidro, E. K., Gee, S., Unda, R., Ma, J., Tsin, A. (2008): Glucose and TGFβ2 Modulate the Viability of Cultured Human Retinal Pericytes and their VEGF Release. Current Eye Research 33: 984-993. doi: 10.1080/02713680802450976.

[39] Musselman, L. P., Fink, J. L., Narzinski, K., Ramachandran, P. V., Hathiramani, S. S., Cagan, R. l., Baranski, T. J. (2011): A High Sugar Diet Produces Obesity and Insulin Resistance in Wild-Type *Drosophila*. Disease Models and Mechanism 4: 842-849. doi: 10.1242/dmm.007948.

[40] Fang, K., Wu, F., Chen, G., Dong, H., Li, J., Zhao, Y., Xu, L., Zou, X., Lu, F. (2019): Diosgenin Ameliorates Palmitic Acid-Induced Lipid Accumulation via AMPK/ACC/CPT-1A and SREBP-1c/FAS Signaling Pathway in LO2 Cells. BMC Complementary and Alternernative Medicine 19: 255. doi: 10.1186/s12906-019-2671-9.

[41] Burgeiro, A., Cerqueira, M. G., Varela-Rodriguez, M. B., Nunes, S., Neto, P., Pereira, F. C., Reis, F., Carvalho, E. (2017): Glucose and Lipid Dysmetabolism in a Rat Model of Prediabetes Induced by a High-Sucrose Diet. Nutrients 9: 638. doi: 10.3390/nu9060638.

[42] Turcotte, L. P., Swenberger, J. R., Yee, A. J. (2002): High Carbohydrate Availability Increases LCFA Uptake and Decreases LCFA Oxidation in Perfused Muscle. American Journal of Physiology Endocrinology and Metabolism 282: E177-E183. doi: 10.1152/ajpendo.00316.2001.

[43] Pimenta, A. S., Gaidu, M. P., Habib, S., So, M., Fediuc, S., Mirpourian, M., Musheev, M., Curi, R., Ceddia, R. B. (2017): Prolonged Exposure to Palmitate Impairs Fatty Acid Oxidation Despite Activation of AMP-Activated Protein Kinase in Skeletal Muscle Cells. Journal of Cellular Physiology 217: 478-485. doi: 10.1002/jcp.21520.

[44] Lu, Z., Qiu, Z. (2017): High Glucose Concentration Restricts Fat Consumption in *Caenorhabditis elegans*. International Journal of Clinical and Experimental Medicine 10: 10554-10559.

[45] Gaster, M., Rustan, A. C., Aas, V., Beck-Nielsen, H. (2004): Reduced Lipid Oxidation in Skeletal Muscle from Type 2diabetic Subjects may be of Genetic Origin: Evidence from Cultured Myotubes. Diabetes 53: 542-548. doi: 10.2337/diabetes.53.3.542.

[46] Lochner, M., Berod, L., Sparwasser, T. (2015): Fatty acid metabolism in the regulation of T cell function. Trends in Immunology 36(2): 81-91. doi.org/10.1016/j.it.2014.12.005.

[47] Bhutada, G., Kavšček, M., Ledesma-Amaro, R., Thomas, S., N. Rechberger, G. N., Nicaud, J., Natter, K: Sugar Versus Fat: Elimination of Glycogen Storage Improves Lipid Accumulation in *Yarrowia lipolytica*. Fems Yeast Research 17: Fox020. doi.org/10.1093/Femsyr/Fox020.

[48] Ardawi, M., Newsholme, E. A. (1982): Maximum Activities of Some Enzymes of Glycolysis, the Tricarboxylic Acid Cycle and Ketone-Body and Glutamine Utilization Pathways in Lymphocytes of the Rat. Biochemical Journal, 208: 743-748. doi: 10.1042/bj2080743.

[49] Rudrappa, S. G., Humphrey, B. D. (2007): Energy Metabolism in Developing Chicken Lymphocytes is Altered During the Embryonic to Posthatch Transition. Journal of Nutrition *137:427-432*. doi.org/10.1093/jn/137.2.427.

[50] de Abreu, L. A., Calixto, C., Waltero, C. F., Della Noce, B. P., Githaka, N. W, Seixas, A., Parizi, L. F., Konnai, S., Vaz Ida, S., Ohashi, K., Logullo, C. (2013): The Conserved Role of AKT/GSK Axis in Cell Survival and Glycogen Metabolism in *Rhipicephalus (Boophilus*) and Microplus Embryo Tick Cell Line BME26. Biochimica Biophysica Acta 1830: 2574-2582. doi.org/10.1016/j.bbagen.2012.12.016.

[51] Varma, S., Lal, B. K., Zheng, R., Breslin, J. W., Saito, S., Pappas, P. J., Hobson II, R. W., Duran, W. N. (2005): Hyperglycemia Alters PI3k and Akt Signaling and Leads to Endothelial Cell Proliferative Dysfunction. American Journal of Physiology. Heart and Circular Physiology 289: H1744-H1751. doi: 10.1152/ajpheart.01088.2004.

[52] Feng, X., Wang, T., Leng, J., Chen, Y., Liu, J., Liu, Y., Wang, W. (2012): Palmitate Contributes to Insulin Resistance through Downregulation of the Src-Mediated Phosphorylation Of Akt In C2C12 Myotubes. Biosci Biotechnol Biochem. 76:1356-1361. doi: 10.1271/bbb.120107.

[53] Wang, L., Liu, X., Zhan, S., Guo, J., Yang, S., Zhong, T., Li, L., Zhang, H., Wang, Y. (2019): Inhibition of GSK3β Reduces Ectopic Lipid Accumulation and Induces Autophagy by the AMPK Pathway in Goat Muscle Satellite Cells. Cells 8: 1378. doi:10.3390/Cells8111378.

[54] Wang, Y., Feng, W., Xue, W., Tan, Y., Heind, W., Li, X. K., Cai, L. (2009): Inactivation of GSK-3β by Metallothionein Prevents Diabetes-Related Changes in Cardiac Energy Metabolism, Inflammation, Nitrosative Damage and Remodeling. Diabetes 58: 1391-1402. doi: 10.2337/db08-1697.

[55] Han, Y., Zeng, F., Tan, G., Yang, C., Tang, H., Luo, Y., Feng J, Xiong H, Guo Q. (2013): Hydrogen Sulfide Inhibits Abnormal Proliferation of Lymphocytes via AKT/GSK3β

Signal Pathway in Systemic Lupus Erythematosus Patients. Cellular Physiology and Biochemistry 31:795-804. doi: 10.1159/000350097.

[56] Neto, R. M., Guimarães S. B., da Silva S. L., da Cruz, J. N, Dias, T., de Vasconcelos P. R. L. (2007): Glutamine or Whey-Protein Supplementation on Alloxan-Induced Diabetic Rats. Effects on $CD4^+$ and $CD8^+$ Lymphocytes. Acta Cirúrgica Brasileira 22: 215-219. doi: 10.1590/s0102-86502007000300010.

[57] Siklova, M., Krauzova, E., Svobodova, B., Kracmerova, J., Stepan, M., Koc, M., Stich, V., Rossmeislova, L. (2019): Circulating Monocyte and Lymphocyte Populations in Healthy First-Degree Relatives of Type 2 Diabetic Patients at Fasting and During Short-Term Hyperinsulinemia. Mediators of Inflammation Article Id 1491083, 7 Pages doi.Org/10.1155/2019/1491083.

[58] Pozzilli, P., Negri, M., Visalli, N., Pagani, S., Beales, P. E., Andreani, D. (1986): Impaired CD4/CD8 Lymphocyte Ratio in Patients with Long Standing Diabetes Mellitus. IRCS Journal of Medical Sciences 14: 648-649.

[59] Al-Sakkaf, L., Pozzilli, P., Tarn, A. C., Schwarz, G., Gale, E. A. M., Bottazzo, G. F. (1989): Persistent Reduction Of CD4/CD8 Lymphocyte Ratio and Cell Activation Before the Onset of Type 1 (Insulin-Dependent) Diabetes Diabetologia 32: 322-325. doi: 10.1007/BF00265550.

[60] Patterson, A. R., Endale, M., Lampe, K., Aksoylar, H. I., Flagg, A., Woodgett, J. R., Hildeman, D., Jordan, M. B., Singh, H., Kucuk, Z., Bleesing, J., Hoebe, K. (2018): Gimap5-Dependent Inactivation of GSK3β is Required for CD4+ T Cell Homeostasis and Prevention of Immune Pathology. Nature Communications. 9: 430. doi: 10.1038/s41467-018-02897-7.

[61] Zhou, B., Zhang, J., Zhang, Q., Permatasari, F., Xu, Y., Wu, D., Yin, Z., Luo, D. (2013): Palmitic Acid Induces Production of Proinflammatory Cytokines Interleukin-6, Interleukin-1β and Tumor Necrosis Factor-A *via* NF-κB-Dependent Mechanism in Hacat Keratinocytes. Mediators of Inflammation: Mediators of Inflammation 2013: 530429. doi: 10.1155/2013/530429.

[62] Perry, B. D., Rahnert, J. A., Xie, Y., Zheng, B., Woodworth-Hobbs, M. E., Price, S. R. (2018): Palmitate-Induced ER Stress and Inhibition of Protein Synthesis in Cultured Myotubes does not Require Toll-Like Receptor 4. Plos One 13: E0191313. doi: 10.1371/journal.pone.0191313.

[63] Shanmugam, N., Reddy, M. A., Guha, M., Natarajan, R. (2003): High Glucose-Induced Expression of Proinflammatory Cytokine and Chemokine Genes in Monocytic Cells. Diabetes 52: 1256-1264. doi: 10.2337/diabetes.52.5.1256.

[64] Panahi, G., Pasalar, P., Zare, M., Rizzuto, R. (2018): High Glucose Induces Inflammatory Responses in HepG2 Cells via the Oxidative Stress-Mediated Activation of NF-κB, and MAPK Pathways in HepG2 Cells. Archives of Physiology and Biochemistry 124: 468-474. doi: 10.1080/13813455.2018.1427764.

[65] Zhang, C., Lu, X., Tan, Y., Li, B., Miao, X., Jin, L., Shi, X., Zhang, X., Miao, L., Li, X., Cai, L. (2012): Diabetes-Induced Hepatic Pathogenic Damage, Inflammation, Oxidative Stress and Insulin Resistance was Exacerbated in Zinc Deficient Mouse Model. Plos One 7: E49257. doi.Org/10.1371/Journal.Pone.0049257.

[66] Datusalia, A. K., Sharma, S. S. (2014): Amelioration of Diabetes-Induced Cognitive Deficits by GSK3β Inhibition is Attributed to Modulation of Neurotransmitters and Neuroinflamm.ation. Molecular Neurobiology 50: 390-405. doi: 10.10007/S12035-014-8632-X.

[67] Turkaly, P., Kerner, J., Hoppel, C. L. (1999): A 22 kDa Polyanion Inhibits Carnitine-dependent Fatty Acid Oxidation in Rat Liver Mitochondria. Febs Letters 460: 241-245. doi.org/10.1016/S0014-5793(99)01354-X.

[68] Lee, K., Kerner, J., Hoppel, C. L. (2011): Mitochondrial Carnitine Palmitoyl transferase 1a (CPT1a) is Part of an Outer Membrane Fatty Acid Transfer Complex. The Journal of Biological Chemistry 286: 25655-25662. doi: 10.1074/jbc.M111.228692.